Manuscript ID: 787
DOI: 10.18462/iir.icr.2019.0787

Experimental Evaluation of a Multi-Ejector Trans-critical CO_2 System for Supermarkets

Simarpreet SINGH[(a)], Armin HAFNER[(b)], Krzysztof BANASIAK[(c)], Prakash M. MAIYA[(a)], Petter NEKSA[(c)]

[(a)]Indian Institute of Technology Madras, 600036, India, simarleo89@gmail.com
[(b)]Norwegian University of Science and Technology, 7491 Trondheim, Norway
[(c)]SINTEF Energy Research Trondheim, 7034 Trondheim, Norway

ABSTRACT

In the present experimental study, the performance of a multi-ejector based trans-critical CO_2 cooling system is tested at high ambient temperature up to 46°C for a supermarket application with and without internal heat exchanger (IHX) and evaporative cooling. The experimental results indicate that the evaporative cooler capacity reaches a maximum at 10 cm pad thickness. However, a very marginal improvement is observed in terms of COP and PIR (Power Input Ratio) for 15 cm pad thickness. Maximum improvement in COP with IHX and evaporative cooler are 11% and 40% respectively. On the other hand, maximum reduction in the system PIR with IHX and evaporative cooler are 8.5% and 26% respectively. However, marginal enhancement in COP and PIR of 4% and 6% are observed respectively with 15 cm cooling pad thickness. From the study, it is evident that the evaporative cooling for the gas cooler of the CO_2 system seems a potential solution to its application at high ambient temperature.

Keywords: Evaporative cooling, COP.

1. INTRODUCTION

CO_2 was proposed as a feasible working fluid for various applications such as automobile air conditioning, residential heating and water heating (Lorentzen, 1994). It is also popular among residential heating applications in cold climates (Richter et al., 2003). However, the implementation of the CO_2 system is not comparable with that of similar systems using synthetic refrigerants in the context of high ambient temperatures due to the unavoidable/inevitable disadvantage of large throttling losses. Potential modifications of the basic vapor compression system to suit tropical ambient temperatures (its operation in cold climates has been proven) to enhance the overall efficiency of the CO_2 system have been reported earlier in the literature. Various modifications suggested to enhance the overall performance of the system for different operating conditions include, two-phase multi-ejectors (Banasiak and Hafner, 2013), internal heat exchanger (IHX) (Se et al., 2017), work recovery expander (Shariatzadeh et al., 2016; Singh and Dasgupta, 2016). Among the various options available and tested, two-phase ejector is considered as a most appropriate option than the latter due to lack of moving parts in the system (Taylor et al., 2007). The pressure lift gained through the ejector results in the reduction of the total workload of the system compressors (Minetto et al., 2013).

Evaporative cooling is one of the most popular technology used in HVAC&R in the last five decades. It is also successfully adopted in numerous applications to improve the heat transfer process. Ball and Visser (2015) used normative evaporative cooling condenser to improve the heat rejection from the gas cooler of a CO_2 refrigeration system. The single and double pass condenser were evaluated. The overall performance of the CO_2 cooling system improves with condensers / gas coolers operating near sub-critical conditions. However, the study was not extended to high ambient temperatures beyond 38°C. The objective of the present experimental study is to evaluate the performance of a multi-ejector based CO_2 cooling system with IHX for varying pad thickness for evaporative cooling of gas cooler at high ambient temperatures up to 46°C for supermarket applications.

2. CO_2 SUPERMARKET TEST-FACILITY LOCATION AND PRESENT AMBIENT CONDITIONS

Fig. 1 shows the location of CO_2 supermarket test-facility/system and ambient conditions during the test. It is installed in southern Asia where the average ambient temperature conditions are high as shown. The location was selected to evaluate the performance of the system for the extreme ambient temperature conditions.

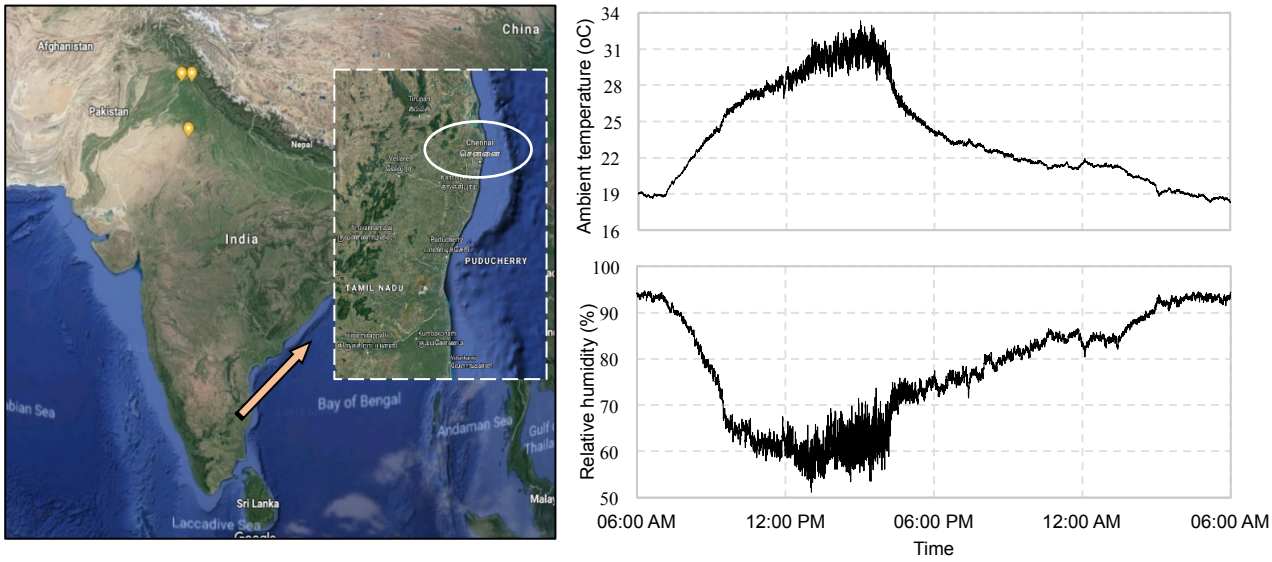

Figure 1: The location of CO_2 supermarket test facility and ambient conditions during the test

3. CO_2 TEST-FACILITY WITH EVAPORATIVE COOLER: A SYSTEM DESCRIPTION

A fully instrumented multi-ejector based CO_2 cooling system test facility for supermarkets is developed and installed at Indian Institute of Technology Madras, India, as shown in Figure 2. It has a total cooling capacity of 33 kW and is designed for supermarket applications, to maintain three different evaporation temperature levels: +6°C (20 kW) for comfort air conditioning (AC), -6°C (10 kW), and -28°C (3 kW) for freezing / food preserving (LT) and for low temperature refrigeration (MT). The test facility is also equipped with a heat recovery system at high temperature with a glycol solution loop to be able to simulate the heat conditions to the evaporators.

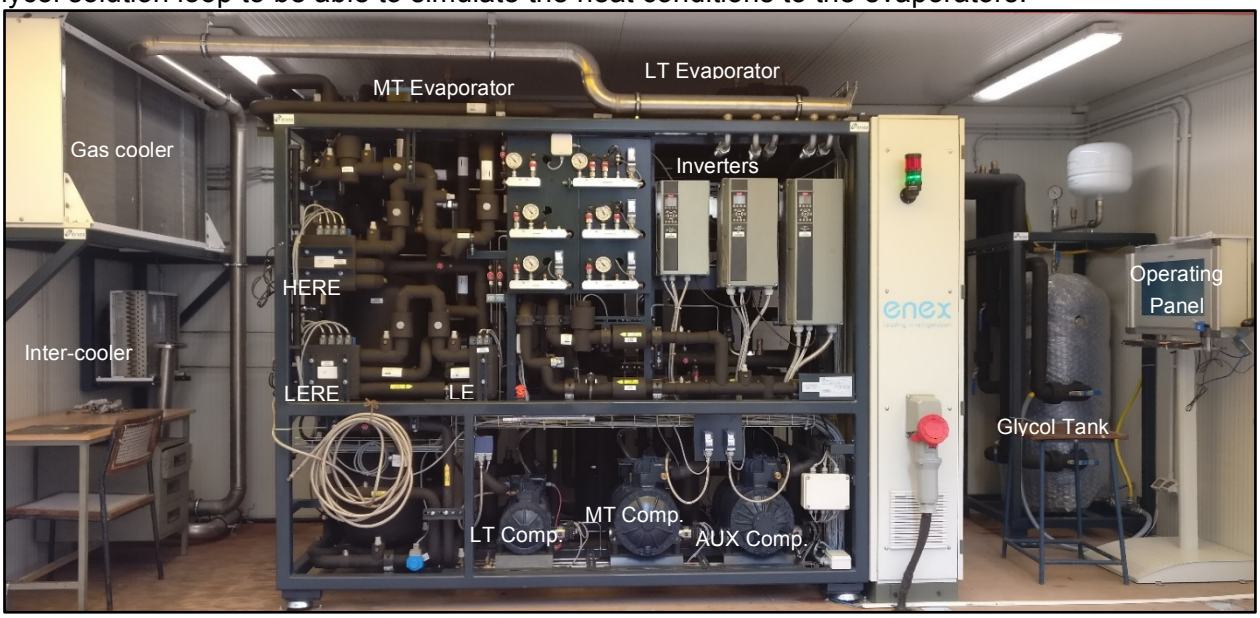

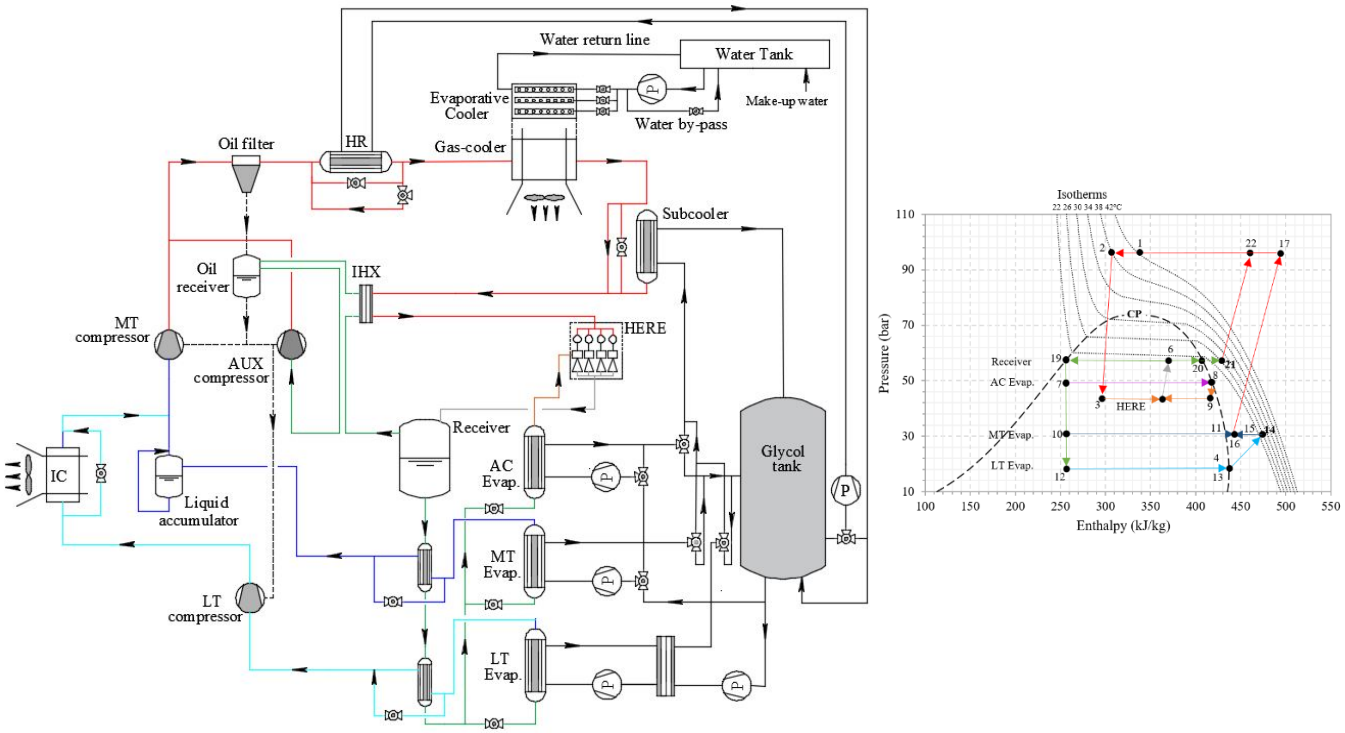

Figure 2: Ejector based CO_2 cooling system test-facility for supermarkets

The two glycol circuits are arranged with different glycol concentrations. LT loop is charged with 55% glycol concentration and the rest of the system which is connected with the glycol tank is charged with 45% glycol concentration in the water. The evaporation temperatures are controlled by suction of the compressors. LT and MT compressors work in tandem with an additional auxiliary (*AUX*) compressor to handle high amounts of flash gas from the receiver. This operates in parallel to the MT compressor, hence the name “parallel compression”. One liquid suction accumulator is also installed to enable the secure separation of liquid and vapor upstream of the compressors to allow a liquid overfeed operation of the evaporators throughout the year. Two ejectors are installed: one with low ejection ratio and a second unit with a high ejection ratio. Multi-ejector with six cartilages with different capacities is used in the test-facility.

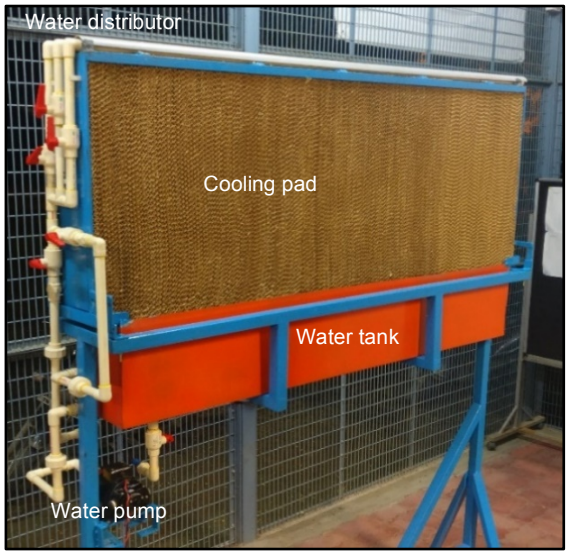

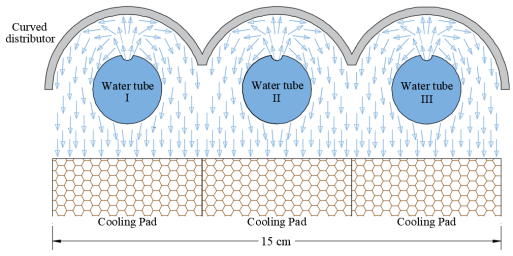

Table 1. Cooling pad details

Details	Units	Value
Face area	m^2	1.157
Cooling pad thickness	cm	5,10,15
Cooling pad design	---	Honeycomb
Water pump capacity	Liters hr^{-1}	1300
Water distribution circuits	---	3

Figure 3: Evaporative cooler with honeycomb cooling pad and water distribution circuit

The operation of switching on/off is taken care by the high pressure (HP) expansion valve opening. The capacity regulation is carried out by on/off switching of the multi-parallel slot ejector cartages. The six cartages with different loads are designed to operate with an individual solenoid valve to

handle different loads. Pressure lifters are also provided in the suction flow entrance to the ejector cartages. The system controllers facilitate both manual and automatic optimization of the gas cooler pressure level with respect to the gas cooler outlet temperature. The facility also has a manual fan controller to vary the airflow rate through the gas cooler to adjust the exit refrigerant temperature. An evaporative cooler with provision to insert up to three honeycomb pads of 5 cm each is positioned in front of the gas cooler. The same fan is made to draw air through this evaporative cooler and the gas cooler as shown in Fig. 2. The evaporative cooling system with three pipes one each to a pad with top holes for even water distribution is shown in Figure 3 and the details are tabulated in Table 1.

4. SUPERMARKET OPERATION

The high pressure CO_2 gas from the gas cooler discharge (state 2) is the motive fluid to the HERE (Fig. 2) and vapour exiting the AC evaporator (state 8) is drawn as the suction fluid to the HERE. HERE lifts CO_2 gas from the low pressure stream (state 8) to higher pressure at the ejector exit (state 6) utilizing high pressure stream (state 2). The receiver separates the two vapour-liquid mixture (state 6). The vapour (state 21) is further compressed in the AUX compressor (state 22) and liquid (state 19) is fed to AC (state 7), MT (state 10) and LT (state 12) evaporators after throttling to the corresponding pressures. The vapor at LT evaporator exit (state 13) is compressed separately up to the suction pressure of the MT compressor (state 14). The LT part of the cycle is not connected with the ejector cycles, which means that the compression takes place from LT evaporator pressure level with no additional boosted pressure lift unlike the other evaporators. Pure vapor (state 11) from the MT evaporator is then mixed with the discharge high pressure vapour of the LT compressor (state 14) and the mixed fluid (state 16) is further compressed by the MT compressor up to the gas cooler pressure (state 17).

4.1. Experimental procedure

The CO_2 circuit side parameters such as temperature of evaporators (AC, LT and MT) receiver pressure (RP), gas cooler outlet temperature, etc. are determined in the test-facility service tool. The gas cooler pressure is automatically optimized according to the gas cooler outlet temperature with the controlling sensor. After directing the system with CO_2 side parameters, the system is turned ON from the main controller (manually). After 15 minutes, the loads of the three evaporators are maintained constant by the secondary water/glycol loop. The loads on the evaporators are controlled by the changing mass flow rate of the glycol solution in the secondary loop. The CO_2 system requires approximately two hours to reach steady state. System performance is evaluated for all steady state conditions using the hourly data and averaged for a single operational temperature. Properties of CO_2 and glycol solution are obtained from REFPROP software and the various operating parameters used for the performance evaluation are tabulated in Table 2. Evaporative cooling system introduced in the CO_2 system is tested for the above 40°C system operating temperature. During the procedure, CO_2 system is set to operate at constant gas cooler outlet temperature by adjusting the gas cooler fan speed manually and keeping it constant. After recording the performance of the system for the set operating temperature, the cooling pad thickness is increased to 5, 10 and 15 cm, one by one allowing the gas cooler outlet temperature to drop at the fixed gas cooler fan speed. The fan speed needs to be reduced manually to achieve the higher gas cooler outlet temperature.

Table 2: CO_2 system operating parameters.

Operating Parameter	Units	Value/Range
Operating temperature	°C	36 to 46
Gas cooler pressure	Bar	80 to 120
Receiver pressure	bar	45
AC Evaporator temperature	°C	+6
LT Evaporator temperature	°C	-28
MT Evaporator temperature	°C	-6

4.2. Performance evaluation

Performance of the ejector based CO_2 cooling system for supermarket applications at high ambient temperature is computed using the following equations.
Efficiency of the evaporative cooler (η_{ec}) is computed by:

$$\eta_{ec} = \frac{T_{inlet\_ec} - T_{outlet\_ec}}{T_{inlet\_ec} - T_{wb}} \quad \text{Eq. (1)}$$

COP of the CO_2 cooling system is computed by,

$$COP = \frac{Q_{AC} + Q_{LT} + Q_{MT}}{P_{AUX} + P_{LT} + P_{MT}} \quad \text{Eq. (2)}$$

Where, load on the three evaporators AC, LT and MT of the system is computed from the glycol side by:

$$\dot{Q}_{AC} = \dot{m}_{AC} * c_p * (T_{AC\_outlet} - T_{AC\_inlet}) \quad \text{Eq. (3)}$$

$$\dot{Q}_{LT} = \dot{m}_{LT} * c_p * (T_{LT\_outlet} - T_{LT\_inlet}) \quad \text{Eq. (4)}$$

$$\dot{Q}_{MT} = \dot{m}_{MT} * c_p * (T_{MT\_outlet} - T_{MT\_inlet}) \quad \text{Eq. (5)}$$

The utility temperatures (T_{UT}) of the three evaporators AC, LT and MT are 22°C, -18°C and 4°C, respectively.

- Power Input Ratio (*PIR*) of the CO_2 cooling system is computed by,

$$PIR = \frac{P_{AUX} + P_{LT} + P_{MT}}{P_{AUX,Carnot} + P_{LT,Carnot} + P_{MT,Carnot}} \quad \text{Eq. (6)}$$

where Carnot power consumption of the three compressors AUX, LT and MT is computed by,

$$P_{AUX,Carnot} = \frac{\dot{Q}_{AC}}{T_{UT\_AC}} * (T_{amb} - T_{UT\_AC}) \quad \text{Eq. (7)}$$

$$P_{LT,Carnot} = \frac{\dot{Q}_{LT}}{T_{UT\_LT}} * (T_{amb} - T_{UT\_LT}) \quad \text{Eq. (8)}$$

$$P_{MT,Carnot} = \frac{\dot{Q}_{MT}}{T_{UT\_MT}} * (T_{amb} - T_{UT\_MT}) \quad \text{Eq. (9)}$$

5. RESULTS AND DISCUSSION

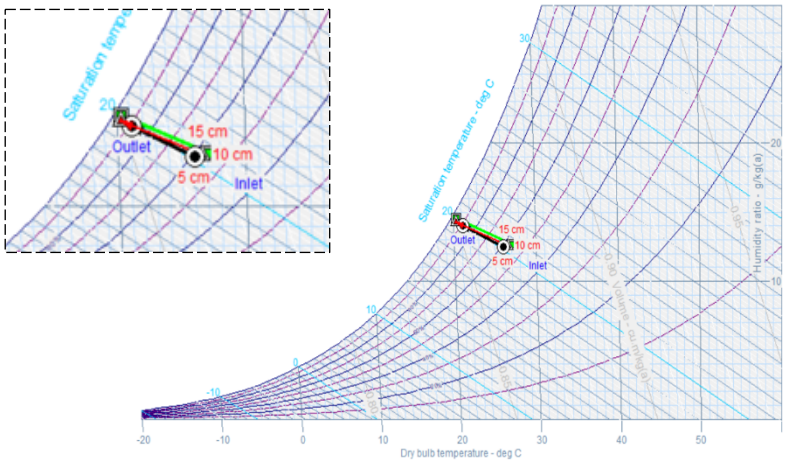

Figure 4: Conditions of air at the inlet and outlet of evaporative cooler on the psychometric chart for 5, 10 and 15 cm thick cooling pad

Fig. 4 shows the conditions of air at the inlet and outlet of evaporative cooler on the psychometric chart for 5, 10 and 15 cm thick cooling pad. The inlet air condition is more or less the same for all the three pad thicknesses as required to compare their performance. It is observed that as the cooling pad thickness increases, relative humidity (RH) increases and dry bulb temperature (DBT) decreases due to increase in the contact surface area between water and cooling pad. However, the law of diminishing returns applies here and the benefit approaches zero when thickness is increased beyond 10 cm.

Fig. 5 shows the evaporative cooler efficiency and evaporative cooler capacity with different cooling pad thickness at various system operating temperatures. It is observed that the efficiency of the evaporative cooler increases with pad thickness at the set gas cooler exit temperature. This is ascribed to the increasing contact surface area between water and air. However, the increment in the evaporative cooler efficiency is only marginal beyond 10 cm cooling pad thickness and the maximum evaporative cooler efficiency observed as 95%. The fan speed had to be set at lower level to achieve higher gas cooler outlet temperature. The resulting lower air velocity increases the residence time and thereby the efficiency increase as the gas cooler exit temperature is set to higher temperatures. Also, pad thickness of 10 cm is observed to be optimum yielding maximum cooler capacity. The pad thickness has two opposing influences; to decrease the face velocity of air due to increase in pressure drop and thereby to increase the cooler efficiency. Hence the same optimum thickness irrespective of the gas cooler exit temperature (set for without evaporative cooling). Within the range of study, the air velocity is the dominant factor governing cooler capacity. Therefore, as the figure indicates, cooler capacity decreases with increase in the set gas cooler temperature where the fan had to be set at lower speeds. Drop in the evaporator cooler capacity is ascribed to the reducing air velocity with respect to the increasing cooling pad thickness beyond 10 cm, which is overall affecting the cooler efficiency. However, as the system operating temperature increases, the evaporator cooler capacity observed decreasing. The maximum capacity observed is 13 kW at 10 cm cooling pad thickness.

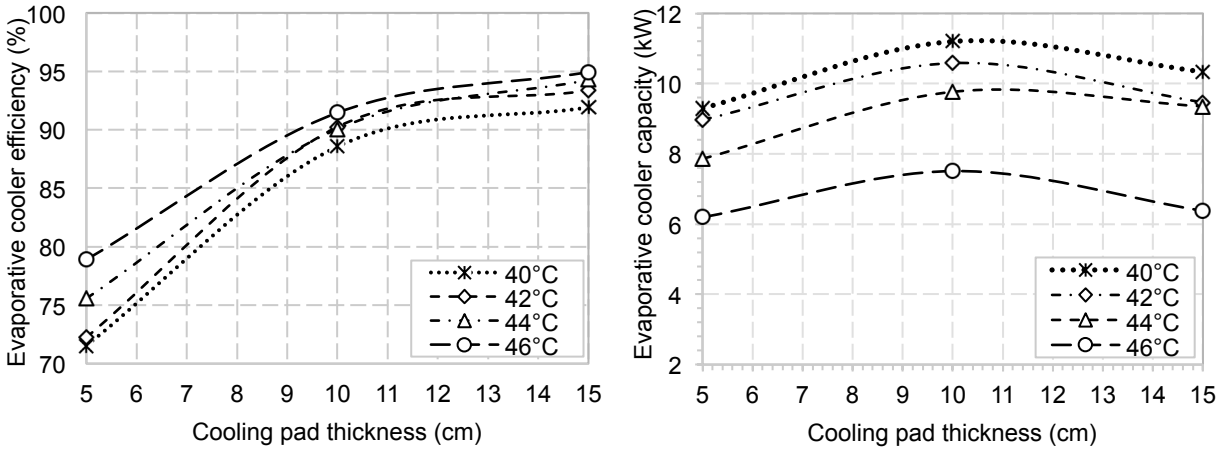

Figure 5: Evaporative cooler efficiency and evaporative cooler capacity with different cooling pad thickness at various system operating temperatures.

Fig. 6 shows the gas cooler outlet temperature and gas cooler capacity with cooling pad thickness at various system operating temperatures. It is observed that as the cooling pad thickness increases, the temperature drop in the gas cooler increases, ascribed to the reduced DBT of air at the inlet of the gas cooler due to the evaporative cooler. As the cooling pad thickness increases, the contact surface area between water and air also increase. Therefore, a progressive reduction in the temperature is observed with respect to increasing cooling pad thickness. However, the gas cooler temperature drop at outlet is marginal beyond 10 cm cooling pad thickness. As the gas cooler outlet temperature decrease, the gas cooler capacity also decreases. Hence, a reduction in cooler capacity is observed as the cooling pad thickness increase. Furthermore, as the system operating temperature increases, the gas cooler capacity also increases. Maximum drop in temperature at gas cooler outlet is ~7K. Also, the maximum gas cooler capacity observed is 34 kW with 5 cm cooling pad thickness at 46°C system operating temperature.

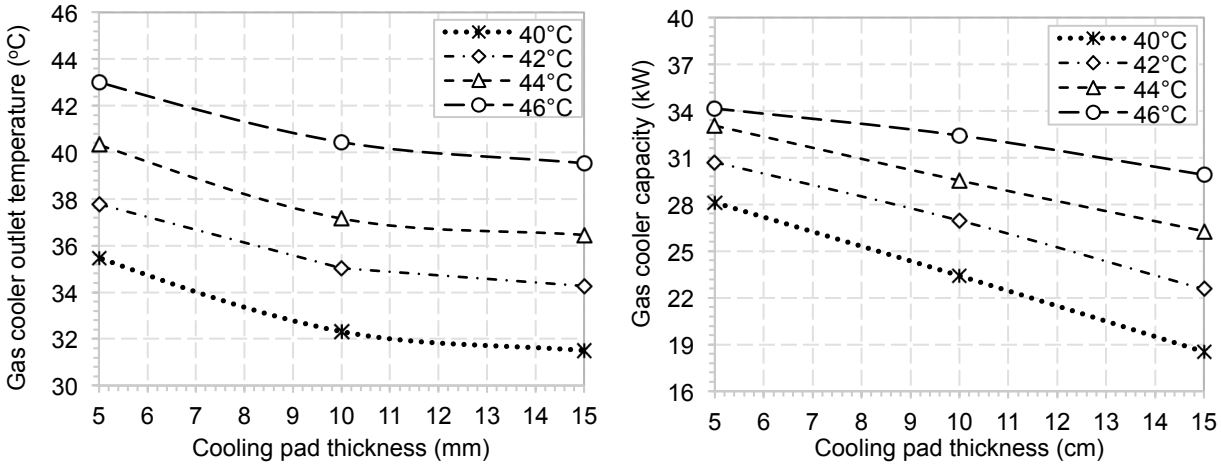

Figure 6: Gas cooler outlet temperature and gas cooler capacity with cooling pad thickness at various system operating temperatures.

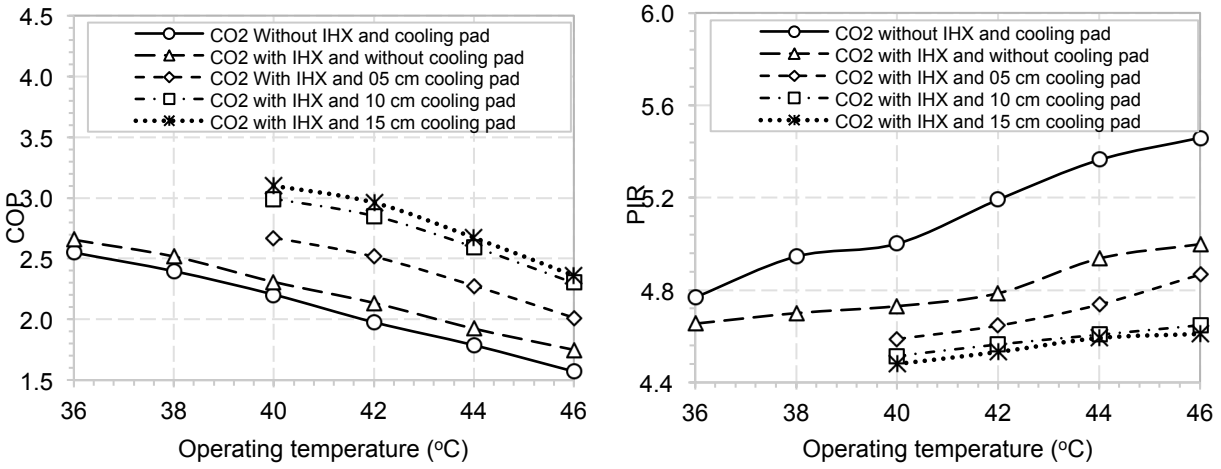

Figure 7: COP and PIR with operating temperatures for CO_2 cooling system with/ without IHX.

Fig. 7 shows the COP and PIR with system operating temperatures for CO_2 cooling system with/ without IHX. It is observed that as the system operating temperature increase, COP of the system decreases and PIR increases. This is due to the increasing system operating gas cooler temperature and pressure at higher operating temperature, which requires more work input to the system. Also, it is observed that, with the use of IHX in the CO_2 system configuration, COP of the CO_2 cooling system improves and PIR reduces. Moreover, with the use of evaporative cooling pad in the system above 40°C, further improvement in the overall performance of the CO_2 cooling system is observed due to reduction in DBT of the air at the gas cooler inlet after crossing the evaporative cooler. From the experimental results, it is also evident that with the increasing cooling pad thickness, the system performance improves further, however, marginal improvement in the overall system performance with the cooling pad thickness beyond 10 cm is observed.

Fig. 8 shows the improvement in COP and reduction in PIR with system operating temperatures. From the experimental results, it is evident that a noteworthy improvement in the overall performance of the CO_2 cooling system is observed with IHX and evaporative cooling in the system configuration. It is observed that, with the support of IHX, maximum COP improvement and PIR reduction are 11% and 8.5% respectively. Moreover, high improvement is observed with the evaporative cooling in CO_2 gas cooler with varying cooling pad thickness. A noteworthy 40% improvement in COP and 26% reduction in system PIR is observed with 15 cm cooling pad thickness. However, a marginal increment in COP and reduction in PIR are 4% and 6% are observed above 10 cm cooling pad thickness.

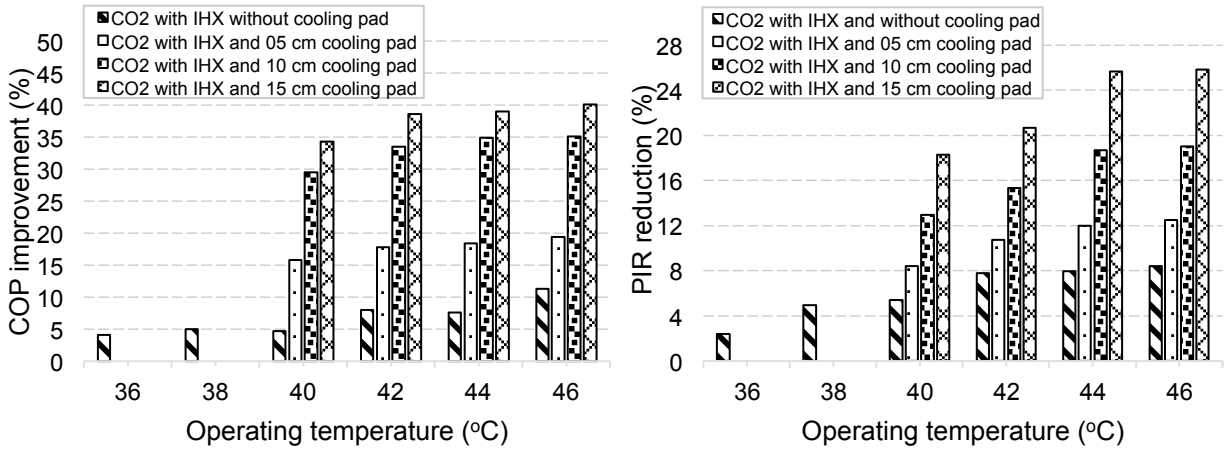

Figure 8: Improvement in COP and reduction in PIR with system operating temperatures

6. CONCLUSIONS

In this experimental study, performance evaluation of a multi-ejector based CO_2 cooling system with/without IHX and evaporative cooling is carried out at high ambient temperature conditions up to 46°C for a supermarket application with different cooling pad thickness. The evaporative cooler is designed, fabricated and tested in the CO_2 cooling system for supermarket application above 40°C with the influence of cooling pad thickness 5, 10 and 15 cm to reduce the gas cooler working pressure in order to improve the overall performance. Evaporative cooling in the CO_2 system configuration appeared as an efficient method to improve the overall performance of the system at high ambient temperature conditions. Experimental results project the maximum evaporative cooler capacity at 10 cm pad thickness, however, very marginal improvement is observed in terms of COP and PIR for 15 cm pad thickness. The maximum improvement in COP with the support of IHX and evaporative cooler are 11% and 40% respectively. On the other hand, the maximum reduction in the system PIR with the support of IHX and evaporative cooler are 8.5% and 26% respectively. Marginal enhancement in COP and PIR observed are 4% and 6% respectively above 10 cm cooling pad thickness. From the present experimental study, it is therefore concluded that, adoption of evaporative cooling in the CO_2 system configuration is a suitable option for supermarket applications for high ambient temperature conditions.

ACKNOWLEDGEMENTS

The research work presented is part of an ongoing Indo-Norwegian project funded by the Ministry of Foreign Affairs, Government of Norway, coordinated by SINTEF, Norway. The Indian authors would like to gratefully acknowledge the additional support received from the Department of Science and Technology (DST) under project: PDF/2017/000083.

REFERENCES

Ball, J., Visser, K., 2015. Applying Evaporative Condensers to Subcritical CO2 Condensing and Transcritical CO2 Gas Cooling, in: Industrial Refrigeration Conference & Exhibition San Diego, California. pp. 1–48.

Banasiak, K., Hafner, A., 2013. Mathematical modelling of supersonic two-phase R744 flows through converging-diverging nozzles: The effects of phase transition models. Appl. Therm. Eng. 51, 635–643.

Lorentzen, G., 1994. Revival of carbon dioxide as a refrigerant. Int. J. Refrig. 17, 292–301.

Minetto, S., Brignoli, R., Banasiak, K., Hafner, A., Zilio, C., 2013. Performance assessment of an off-the-shelf R744 heat pump equipped with an ejector. Appl. Therm. Eng. 59, 568–575.

Richter, M.R., Song, S.M., Yin, J.M., Kim, M.H., Bullard, C.W., Hrnjak, P.S., 2003. Experimental results of transcritical CO2heat pump for residential application. Energy 28, 1005–1019.

Se, M., Hoon, D., Soo, M., Kim, M., 2017. Investigation on the optimal control of gas cooler pressure for a CO 2 refrigeration system with an internal heat exchanger. Int. J. Refrig. 77, 48–59.

Shariatzadeh, O.J., Abolhassani, S.S., Rahmani, M., Nejad, M.Z., 2016. Comparison of transcritical CO2 refrigeration cycle with expander and throttling valve including/excluding internal heat exchanger : Exergy and energy points of view. Appl. Therm. Eng. 93, 779–787.

Singh, S., Dasgupta, M.S., 2016. Evaluation of research on CO2 trans-critical work recovery expander using multi attribute decision making methods. Renew. Sustain. Energy Rev. 59, 119–129.

Taylor, P., House, M., Street, M., Wt, L., Groll, E.A., Kim, J., 2007. Review of Recent Advances toward Transcritical CO2 Cycle Technology. HVAC&R Res. 13, 499–520.